

Non-Markovianity and memory enhancement in Quantum Reservoir Computing

Antonio Sannia,^{*} Ricard Ravell Rodríguez,[†] Gian Luca Giorgi, and Roberta Zambrini
*Institute for Cross-Disciplinary Physics and Complex Systems (IFISC) UIB-CSIC,
 Campus Universitat Illes Balears, 07122, Palma de Mallorca, Spain.*

Featuring memory of past inputs is a fundamental requirement for machine learning models processing time-dependent data. In quantum reservoir computing, all architectures proposed so far rely on Markovian dynamics, which, as we prove, inherently lead to an exponential decay of past information, thereby limiting long-term memory capabilities. We demonstrate that non-Markovian dynamics can overcome this limitation, enabling extended memory retention. By analytically deriving memory bounds and supporting our findings with numerical simulations, we show that non-Markovian reservoirs can outperform their Markovian counterparts, particularly in tasks that require a coexistence of short- and long-term correlations. We introduce an embedding approach that allows a controlled transition from Markovian to non-Markovian evolution, providing a path for practical implementations. Our results establish quantum non-Markovianity as a key resource for enhancing memory in quantum machine learning architectures, with broad implications in quantum neural networks.

Introduction.— Within the field of machine learning, there is growing interest in neural networks capable of processing time-dependent data presenting long-range correlations [1]. Architectures such as long short-term memory [2] and transformers [3] are currently producing outstanding results in time series forecasting and language processing. However, the high energy cost of these deep learning models is a significant limiting factor for their scalability [4–7]. As a promising alternative, analog implementations of machine learning models offer a potential solution to this challenge [8–10].

In this context, Reservoir Computing [11, 12] has attracted significant attention due to its versatility in handling both static and temporal tasks, its training efficiency (requiring only linear regression), and its adaptability to diverse physical platforms without the need for fine-tuning of experimental parameters [13]. Among the various proposals [12], quantum systems allow the exploration of unique possibilities such as having an exponential number of degrees of freedom and direct embedding of quantum inputs without the need for tomography [14, 15]. Several works have been done to connect the performances of quantum reservoir computing (QRC) to physical properties such as dynamical phase transitions [16, 17], quantum dissipation [18–20], quantum chaos [21], squeezing [22], topological effects [23], entanglement [24], quantum back-action [25, 26] and quantum coherences [27].

One of the key features of QRC is the presence of an internal memory, which enables the processing of temporal information, a critical capability for tasks such as time series analysis and forecasting [15]. The specific memory featured by the reservoir in its dynamics is therefore a fundamental resource for QRC, and a complete characterization of it is still missing. In the following, we address this fundamental question by showing that all

reservoir models proposed so far, relying on a Markovian evolution, inevitably erase information about past inputs at an exponential rate. In fact, while Markovian reservoir models enable the inference of unlimited data streams and allow for memory adjustment [18, 28], their exponential memory decay fundamentally restricts their applicability. Importantly, we identify quantum non-Markovianity as the key mechanism to overcome this limitation, opening the possibility of studying problems where longer memory is needed.

Quantum non-Markovianity refers to the phenomenon in which the evolution of an open quantum system shows significant memory effects, so that its future behavior depends not only on its current state but also on its past history [29–33]. This can lead to revivals of coherence, entanglement, and other quantum properties that would otherwise decay [34–37]. The mathematical characterization of various aspects of non-Markovianity has been an active area of research in recent years, and its role as a resource in quantum technologies has been shown to be highly context-dependent. It has been shown to be beneficial in quantum metrology [38], control [39], teleportation [40], information processing [41], computing [42], and entanglement generation [43]. However, it can also be detrimental in certain scenarios, such as inhibiting the emergence of synchronization [44] and negatively impacting specific classes of quantum algorithms [45].

In this Letter, we demonstrate how non-Markovianity can enhance memory and, consequently, the performance of QRC. Specifically, we provide theoretical justifications and support our claims with both analytical and numerical results. Additionally, we propose potential implementations where non-Markovianity can be introduced and controlled through an embedding method [31].

Memory bounds of Markovian reservoirs.— The Gorini-Kossakowski-Sudarshan-Lindblad (GKLS) Master Equation [46, 47]

$$\frac{d\rho}{dt} = \mathcal{L}[\rho] = -i[H, \rho] + \sum_i \gamma_i \left(L_i \rho L_i^\dagger - \frac{1}{2} \{L_i^\dagger L_i, \rho\} \right),$$

^{*} sannia@ifisc.uib-csic.es

[†] ricard@ifisc.uib-csic.es

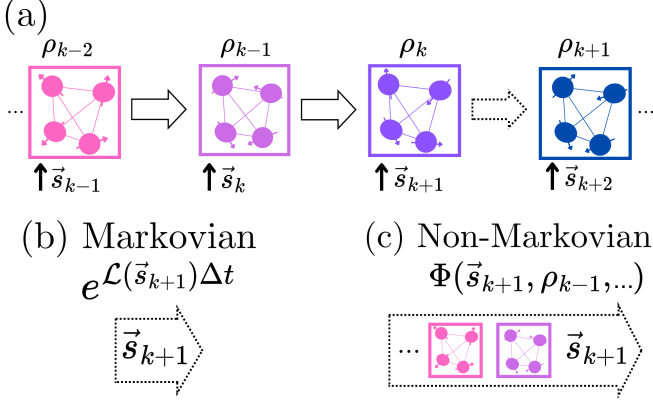


FIG. 1. Scheme of a reservoir evolution (a). In the Markovian case (b), the reservoir state updating rule depends solely on the injected input, whereas in the non-Markovian one (c), past states also play a role.

is known to describe the Markovian evolution of an open system with Hamiltonian H , where $\{L_i\}$ are the jump operators describing the interaction with the external environment, and $\{\gamma_i\}$ are the decay rates. In QRC, the reservoir (an open quantum system) is driven by an input sequence, while a set of measured observables form the output, in a three-layer configuration (see [15, 48]). Given time series of input vectors $\{\dots, \vec{s}_{k-1}, \vec{s}_k, \vec{s}_{k+1}, \dots\}$, where k iterates over the time-steps, a Markovian quantum reservoir state evolves according to the rule:

$$\rho_{k+1} = e^{\mathcal{L}(\vec{s}_{k+1})\Delta t} \rho_k \quad (1)$$

where $\mathcal{L}(\vec{s}_{k+1})$ is a parametric Liouvillian that defines the particular reservoir model and Δt is the evolution time, which can be considered as a model hyperparameter (see Fig. 1 (b)).

After each input injection, the reservoir response is optimized for the target task, with a simple linear regression of observable expectation values. In particular, considering a set of observables $\{\mathcal{O}_i\}$, the reservoir output y_k is given by the expression:

$$y_k = \omega_0 + \sum_i \omega_i \text{Tr}\{\rho_k \mathcal{O}_i\}, \quad (2)$$

where the coefficients ω_i are optimized, in a supervised way, depending on the problem of interest [13].

For the proper operation of a reservoir computing model, different properties need to be satisfied, such as the echo state property [49]. This means that the reservoir will produce the same outcome independently of the initial state if the same input series is injected. The echo state property holds for any input sequence if the stationary state $\mathcal{L}(\vec{s}_k)$ is unique for every input \vec{s}_k [18]. The converse implication is straightforward to verify. In the following, we will restrict to Liouvillians satisfying this condition. Moreover, if $\mathcal{L}(\vec{s}_k)$ is a continuous function

of \vec{s}_k , then the reservoir state will depend only on the recent input history, satisfying the so-called fading memory [18]. Under the fading memory property, each output y_k can be considered a time-invariant function and, consequently, can be expanded according to a Volterra series [50]. In our notation, the Volterra expansion takes the following form:

$$\begin{aligned} y_k &= \sum_{n=1}^{\infty} \prod_{\tau_1=0}^{\infty} \prod_{\tau_2=\tau_1}^{\infty} \cdots \prod_{\tau_n=\tau_{n-1}}^{\infty} \mathcal{P}_1(\vec{s}_{k-\tau_1}) \cdots \mathcal{P}_n(\vec{s}_{k-\tau_n}) \\ &= \sum_{n=1}^{\infty} f_n(\vec{s}_{k-\tau_1}, \dots, \vec{s}_{k-\tau_n}) \end{aligned} \quad (3)$$

where $\mathcal{P}_i(\vec{s}_{k-\tau_i})$ are polynomials of degree one with respect to the $\vec{s}_{k-\tau_i}$ entries, and f_n are functionals that group all the monomials in the series that have input dependence up to a delay τ_n .

Given a Markovian QRC with reservoir dynamics governed by Eq. (1), we show in the Supplemental material (see Ref. [48]) that for each element of the output Volterra expansion

$$|f_n(\vec{s}_{k-\tau_1}, \dots, \vec{s}_{k-\tau_n})| = \mathcal{O}(e^{-a\tau_n}), \quad (4)$$

where a is a positive constant that depends on the particular reservoir model. Importantly, Eq. (4) implies fundamental bounds on the reservoir memory. Considering a T steps evolution, we quantify the reservoir's ability to reproduce past input functionals with the capacity introduced in Ref. [51]:

$$C[\hat{y}] = 1 - \min_{\{\omega_i\}} \frac{MSE_T[\hat{y}]}{\langle y^2 \rangle_T}, \quad (5)$$

where $\{\hat{y}_k\}_{k=1}^T$ is the target series; MSE indicates the mean square error: $MSE_T = \sum_{k=1}^T (\hat{y}_k - y_k)^2 / T$ (depending on the weights in Eq. (2)); and $\langle y^2 \rangle_T = \sum_{k=1}^T y_k^2 / T$.

Among the properties of the capacity [51], we recall that $0 \leq C \leq 1$, where the extreme cases $C = 0$ and $C = 1$ correspond to a complete mismatch between the target and predictions, and to a perfect agreement, respectively. Combining now Eqs. (4) and (5), and considering a target $\hat{y}(\tau)$ that is a function only of past inputs delayed by a certain τ (e.g. $\hat{y}_k(\tau) = \vec{s}_{k-\tau}^2$) we find the following capacity scaling:

$$C[\hat{y}(\tau)] = \mathcal{O}(e^{-a\tau}). \quad (6)$$

The interpretation of Eq. (6) is that a Markovian reservoir tends to *exponentially* erase information of past inputs over time. This conclusion can be directly generalized in the case in which the inputs, instead of being vectors of classical parameters, are quantum states, making the presented considerations valid even for quantum tasks.

As we will show below, for some kinds of tasks, a longer memory is required, and the introduction of quantum

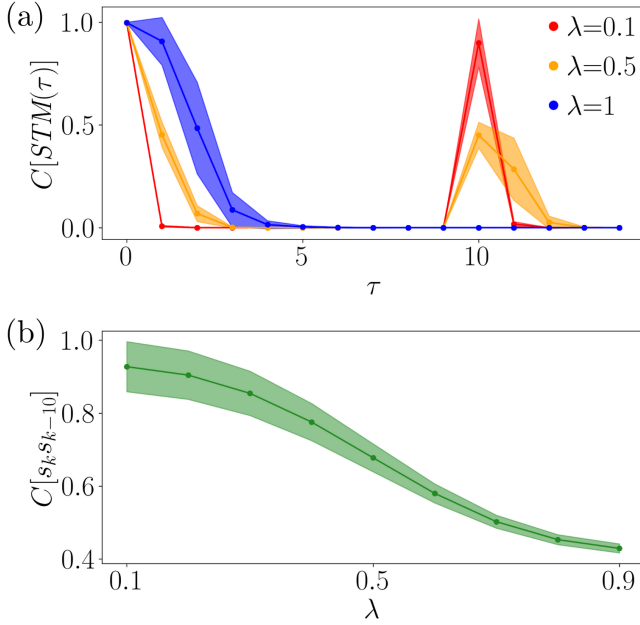


FIG. 2. Quantum Residual Reservoir performance analysis. (a) Capacity for the short-term memory task, as a function of the delay τ . (b) Capacity of reproducing the monomial $s_k s_{k-10}$, varying λ in steps of 0.1. All the capacity values have been averaged over 100 random realizations of reservoir initial states, Hamiltonian couplings, and input sequences [48]. The hyperparameters have been fixed to be $N = 3$, $\Delta t = 10$, $h = 1$ and $\gamma = 0.1$.

non-Markovianity is necessary for overcoming this exponential decay. In particular, we introduce a more general class of quantum reservoir computers whose updating rule is

$$\rho_{k+1} = \Phi(\vec{s}_{k+1}, \rho_{k-1}, \dots) \rho_k, \quad (7)$$

where Φ is a super-operator corresponding to a non-Markovian physical process in which an external environment has a memory of the previous reservoir states (see Fig. 1 (c)).

Quantum Residual Reservoir. – We now give an illustrative example of a non-Markovian process that allows us to overcome the exponential scaling previously found. For generic Markovian reservoir, defined from a Liouvillian $\mathcal{L}(\vec{s}_k)$, we can always define a fading memory time scale τ_{FM} such that all the delayed inputs $\vec{s}_{k-\tau}$, with $\tau > \tau_{FM}$, are practically irretrievable from the reservoir state ρ_k [18, 25]. Let us consider instead the following non-Markovian QRC evolution:

$$\rho_{k+1} = e^{\mathcal{L}(\vec{s}_{k+1})\Delta t} [\lambda \rho_k + (1 - \lambda) \rho_{k-\tau_E}], \quad (8)$$

where λ is a model hyperparameter that takes values in the interval $[0, 1]$, and τ_E is the non-Markovian environment time scale, which we consider to be larger than τ_{FM} . Interestingly, Eq. (8) represents a quantum counterpart of the recently introduced Residual reservoir computers [52], making use of dilated skip connections [53].

For this non-Markovian case, it is now immediate to see that the state ρ_k is statistically correlated with the past inputs following an exponential decay trend, inside the fading memory window of $\mathcal{L}(\vec{s}_k)$, meanwhile, for inputs delayed from a factor at least equal to τ_E , we find an information retrieval that overcomes the fading memory time. Importantly, the parameter λ governs the interplay between these competing behaviors –the Markovian loss of input information and the non-Markovian revival–with its optimal value being task-dependent.

To numerically verify the memory properties of this Quantum Residual Reservoir, we start from the Markovian model introduced in Ref. [18]. Specifically, considering the input sequence to be composed of scalar values $s_k \in [0, 1]$, the parametric Liouvillian will act according to the equation

$$\mathcal{L}(s_k)[\rho] = -i[H(s_k), \rho] + \mathcal{D}_L[\rho], \quad (9)$$

where $H(s_k)$ is an input-dependent Hamiltonian that reads

$$H = \sum_{i < j}^N J_{ij} \sigma_i^x \sigma_j^x + h \sum_{i=1}^N \sigma_i^z + h(s_k + 1) \sum_{i=1}^N \sigma_i^x, \quad (10)$$

where N is the number of reservoir qubits, J_{ij} are the random couplings, sampled from the fixed interval $[-1, 1]$, h is the strength of the magnetic fields, and \mathcal{D}_L is a local dissipator:

$$\mathcal{D}_L[\rho] \equiv \gamma \sum_{i=1}^N (\sigma_i^- \rho \sigma_i^+ - \frac{1}{2} \{\sigma_i^+ \sigma_i^-, \rho\})$$

where γ is its corresponding decay rate.

We can now study the Quantum Residual Reservoir's ability to retrieve past inputs by computing the performance for the short-term memory task (STM) [54]. According to the standard definition, at each time step, the target values \hat{y}_k are the past inputs delayed by a time τ : $\hat{y}_k = s_{k-\tau}$, while the injected inputs are randomly extracted from the interval $[0, 1]$. Fixing $\tau_E = 10$ and considering the output observables to be the single-qubit matrices $\{\sigma_i^z\}_{i=1}^N$, in Fig. 2 (a) we plot the estimated capacity as a function of the delay τ for different values of λ [48]. As predicted by the theoretical results, when the evolution is Markovian ($\lambda = 1$), the capacity exhibits a typical decay, making inputs delayed by $\tau > 3$ practically irretrievable. Moreover, as expected in the non-Markovian cases ($\lambda = 0.5$ and $\lambda = 0.1$), we observed a capacity revival at $\tau = \tau_E$, whose magnitude increases as λ decreases.

This memory revival, observed exclusively in non-Markovian dynamics, can be crucial for solving certain tasks. For instance, Fig. 2 (b) illustrates that the Quantum Residual Reservoir's capacity for the target $\hat{y}_k = s_k s_{k-10}$ tends to decrease with λ [48]. This behavior suggests that the task requires the reservoir to retain both recent inputs (s_k) and long-delayed ones (s_{k-10}). Achieving this dual time-scale memory is only possible by introducing non-Markovianity. While in this synthetic QRC

design, the performance in the chosen non-linear memory task is monotonically related to the revival strength, in general, the form of dissipation and non-Markovianity cannot be isolated, and moreover different memory forms are required in different tasks. Therefore, the enhancing effect of non-Markovianity will depend on the QRC task.

Embedded Non-Markovian reservoir.— Non-Markovian dynamics of open quantum systems can be obtained from a Markovian evolution in a larger space, tracing out some degrees of freedoms [31, 55–61]. We will follow this approach, known as embedding method [31], for assessing the memory and forecasting of QRC tuned from a Markovian to non-Markovian operation. We consider as a reservoir the open quantum system model of Ref. [62], whose evolution rule can be factorized in the following form:

$$\rho_{k+1} = \Phi \circ e^{\mathcal{L}(s_k)\Delta t}[\rho_k],$$

where $\mathcal{L}(s_k)$ is the same Liouvillian of Eq. (9) and Φ is a non-Markovian channel that involves the presence of auxiliary qubits. In particular, given the quantum reservoir in Eq. (10), we couple each of the N qubits to an auxiliary one to implement the Φ action (see supplementary material for a schematic representation of the model [48]). First of all, at each time step k , each pair of auxiliary and reservoir qubits interact with a partial Swap operation

$$\hat{P}_i(\eta) = \cos(\eta)\mathbb{I} + i\sin(\eta)\hat{S}_i$$

where i is an index ranging from 1 to N ; \mathbb{I} represents the identity operator over the entire space generated by the $2N$ qubits; \hat{S}_i denotes the Swap operator acting on the i th qubits of the reservoir and the auxiliary system; and η is a hyperparameter in the set $[0, \pi/2)$, interpreted as the interaction strength between the system and the auxiliary qubits. After the application of all the partial Swaps, a set of depolarizing channels acts on the auxiliary system:

$$\Delta_\Omega^i[\rho] = \sum_{m=0}^3 \hat{K}_i^m \rho \hat{K}_i^{m\dagger},$$

where \hat{K}_i^m are the Kraus operators acting on the i -th auxiliary qubit: $\hat{K}_i^0 := \sqrt{1 - 3\Omega/4}\mathbb{I}_i$, $\hat{K}_i^1 := \sqrt{\Omega/4}\sigma_i^x$, $\hat{K}_i^2 := \sqrt{\Omega/4}\sigma_i^y$, $\hat{K}_i^3 := \sqrt{\Omega/4}\sigma_i^z$, and $0 \leq \Omega \leq 1$.

Importantly, Ω represents the strength of the depolarizing channels and allows tuning the non-Markovianity level. In particular, in the case of $\Omega = 1$, the reservoir dynamics is fully Markovian because the auxiliary system, at each time step, will be prepared to a fully mixed state, having no memory of past reservoir states. On the other hand, as shown in Ref. [62], it is expected that decreasing the Ω value corresponds to an increase of non-Markovianity, up to the maximum case for $\Omega = 0$, where the partial Swap is applied with auxiliary qubits in the state of the previous step leading to the maximum back-flow of memory in the system. In the supplementary material, we show a numerical verification of this behavior [48].

Turning now to QRC tasks, we examine how non-Markovianity influences the reservoir capabilities of chaotic time series forecasting, while the performance in other tasks is presented in Ref. [48]. Specifically, we focus on the widely studied Mackey-Glass (MG) series [63], where the target values satisfy the delayed differential equation:

$$\dot{s}(t) = -0.1s(t) + \frac{0.2s(t - \tau)}{1 + s(t - \tau)^{10}}, \quad (11)$$

and we set $\tau = 17$ to ensure a chaotic regime [64, 65]. During the training phase, we fed the system with the numerical solution of Eq. (11), solved with a time resolution of $t_r = 3$ (see Ref. [66] for details), with input values rescaled to the interval $[0, 1]$. The output coefficients are trained to perform a one-step-ahead prediction task, $\hat{y}_k = s_{k+1}$ [48], using measured observables that correspond to Pauli strings of length one (σ_i^a) and two ($\sigma_i^a \sigma_j^b$), where $a, b \in \{x, y, z\}$ and $1 \leq i, j \leq N$ with $i \neq j$. Finally, during the evaluation phase, the system evolved autonomously, using its previous output as the current input at each time step.

In Fig. 3, we present the reservoir predictions during the test phase for different values of Ω . The results clearly indicate that the best forecast occurs in the non-Markovian regime with $\Omega = 0.5$, outperforming the fully Markovian one obtained for $\Omega = 1$. Moreover, as expected, the degree of non-Markovianity in the updating rule must be tuned to achieve an advantage. Notably, when $\Omega = 0$, corresponding to the maximum amount of non-Markovianity, the reservoir's forecasting ability deteriorates.

As anticipated, the potential performance gains from introducing non-Markovianity depend on the specific task at hand. Looking at the linear short-term memory (see results in Ref. [48]), non-Markovianity ($\Omega \neq 1$) generally introduces non-monotonous linear memory decay, enhancing the performance at long times, but can be detrimental at short times. Looking instead at a different forecasting task, non-Markovianity does not yield any improvement for the Santa Fe laser task [67] (in Ref. [48]). One possible explanation is that, in this task, the system is not intended to evolve autonomously (as in the Mackey-Glass task, as the reservoir is continuously driven by the true series values, potentially making the prediction problem inherently easier).

Moreover, the non-Markovian embedding we present is not restricted to the specific choice of interaction considered (the partial Swap unitary in this case) or to the use of depolarizing channels (e.g. dissipative channels can be also considered). Alternative schemes can be readily constructed using experimentally available quantum gates, such as entangling operations [28, 68, 69], or by employing other implementable noise models like amplitude damping [18, 70], making our approach broadly applicable across different physical platforms.

Conclusions.— We have established fundamental limitations on memory capacity in Markovian QRC and

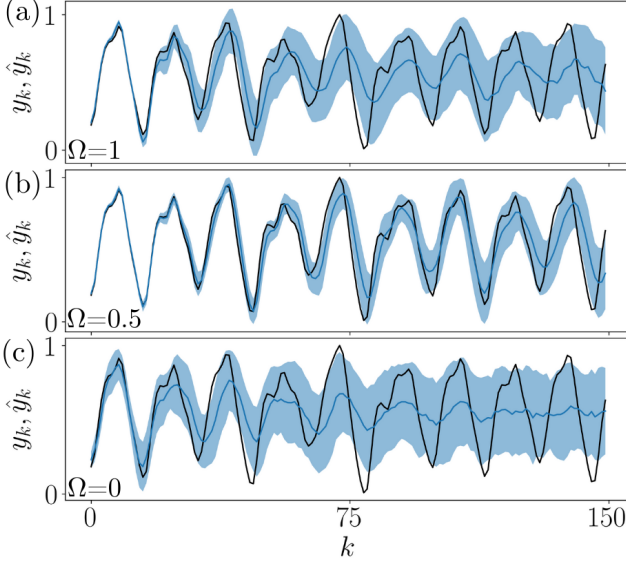


FIG. 3. Reservoir predictions of the Mackey-Glass time-series during a test phase of 150 points. The black lines correspond to the numerical solutions of the Mackey-Glass equation, while the blue lines are the average of predictions over 100 random realizations of reservoir initial states and Hamiltonian couplings [48]. The blue shadow regions are the statistical errors, chosen as one standard deviation. Different Ω values have been considered for changing the non-Markovianity amount: (a) $\Omega = 1$, (b) $\Omega = 0.5$, (c) $\Omega = 0$. The other hyperparameters have been fixed to the following values: $h = 1$, $dt = 0.5$, $\gamma = 0.1$, $\eta = \pi/4$, and $2N = 8$. The performances have been quantified through the average mean square error between the numerical solution of the Mackey-Glass equation and the reservoir predictions, taking 150 points in the test phase. The values found, in descending order with respect to Ω , are respectively $1.8 \cdot 10^{-2}$, $6.8 \cdot 10^{-3}$, and $2 \cdot 10^{-2}$.

demonstrated how non-Markovianity can enhance memory retention. Our results show that Markovian reservoirs inevitably experience an exponential decay of past

memory, restricting their information capacity for long-term dependencies. By incorporating non-Markovian dynamics in an illustrative example, we have demonstrated an extension of the reservoir’s memory through a revival mechanism and the enhancing effect in a non-linear memory task requiring long-range correlations. While in this case the performance improvement is monotonous in the revival strength, this is not the common situation. With an embedding approach enabling the controlled introduction of non-Markovianity in QRC, we showed that non-Markovian reservoirs can outperform their Markovian counterparts in chaotic time series forecasting, illustrating the practical benefits of memory effects in quantum machine learning. Our results establish non-Markovianity as a resource for QRC, with broader implications in quantum information processing. An open, challenging question is to establish a comprehensive theoretical framework in QRC to relate reservoirs’ memory and non-Markovianity to their performance on different temporal tasks.

ACKNOWLEDGEMENTS

We acknowledge the Spanish State Research Agency, through the María de Maeztu project CEX2021-001164-M funded by the MCIU/AEI/10.13039/501100011033, through the COQUSY project PID2022-140506NB-C21 and -C22 funded by MCIU/AEI/10.13039/501100011033, MINECO through the QUANTUM SPAIN project, and EU through the RTRP - NextGenerationEU within the framework of the Digital Spain 2025 Agenda. The CSIC Interdisciplinary Thematic Platform (PTI+) on Quantum Technologies in Spain (QTEP+) is also acknowledged. The project that gave rise to these results received the support of a fellowship from the “la Caixa” Foundation (ID 100010434). The fellowship code is LCF/BQ/DI23/11990081.

-
- [1] B. Lim and S. Zohren, *Time-series forecasting with deep learning: a survey*, Philosophical Transactions of the Royal Society A: Mathematical, Physical and Engineering Sciences **379**, 20200209 (2021).
 - [2] S. Hochreiter and J. Schmidhuber, *Long short-term memory*, Neural Computation **9**, 1735 (1997).
 - [3] A. Vaswani, N. Shazeer, N. Parmar, J. Uszkoreit, L. Jones, A. N. Gomez, L. Kaiser, and I. Polosukhin, *Attention is all you need*, arxiv:1706.03762 (2023).
 - [4] R. Desislavov, F. Martínez-Plumed, and J. Hernández-Orallo, *Trends in AI inference energy consumption: Beyond the performance-vs-parameter laws of deep learning*, Sustainable Computing: Informatics and Systems **38**, 100857 (2023).
 - [5] S. Samsi, D. Zhao, J. McDonald, B. Li, A. Michaleas, M. Jones, W. Bergeron, J. Kepner, D. Tiwari, and V. Gadepally, in *2023 IEEE High Performance Extreme Computing Conference (HPEC)* (IEEE, 2023) p. 1–9.
 - [6] L. F. W. Anthony, B. Kanding, and R. Selvan, *Carbon-tracker: Tracking and predicting the carbon footprint of training deep learning models*, arXiv:2007.03051 (2020).
 - [7] J. Park, M. Naumov, P. Basu, S. Deng, A. Kalaiah, D. Khudia, J. Law, P. Malani, A. Malevich, S. Nadathur, J. Pino, M. Schatz, A. Sidorov, V. Sivakumar, A. Tulloch, X. Wang, Y. Wu, H. Yuen, U. Diril, D. Dzhulgakov, K. Hazelwood, B. Jia, Y. Jia, L. Qiao, V. Rao, N. Rotem, S. Yoo, and M. Smelyanskiy, *Deep learning inference in facebook data centers: Characterization, performance optimizations and hardware implications*, arXiv:1811.09886 (2018).
 - [8] D. Marković, A. Mizrahi, D. Querlioz, and J. Grollier, *Physics for neuromorphic computing*, Nature Reviews Physics **2**, 499–510 (2020).

- [9] L. G. Wright, T. Onodera, M. M. Stein, T. Wang, D. T. Schachter, Z. Hu, and P. L. McMahon, *Deep physical neural networks trained with backpropagation*, *Nature* **601**, 549–555 (2022).
- [10] M. Hu, C. E. Graves, C. Li, Y. Li, N. Ge, E. Montgomery, N. Davila, H. Jiang, R. S. Williams, J. J. Yang, Q. Xia, and J. P. Strachan, *Memristor-based analog computation and neural network classification with a dot product engine*, *Advanced Materials* **30** (2018).
- [11] K. Nakajima, *Physical reservoir computing—an introductory perspective*, *Japanese Journal of Applied Physics* **59**, 060501 (2020).
- [12] I. F. Kohei Nakajima, *Reservoir Computing: Theory, Physical Implementations, and Applications* (Springer Singapore, 2021).
- [13] M. Cucchi, S. Abreu, G. Ciccone, D. Brunner, and H. Kleemann, *Hands-on reservoir computing: a tutorial for practical implementation*, *Neuromorphic Computing and Engineering* **2**, 032002 (2022).
- [14] K. Fujii and K. Nakajima, *Harnessing disordered-ensemble quantum dynamics for machine learning*, *Physical Review Applied* **8** (2017).
- [15] P. Mujal, R. Martínez-Peña, J. Nokkala, J. García-Beni, G. L. Giorgi, M. C. Soriano, and R. Zambrini, *Opportunities in quantum reservoir computing and extreme learning machines*, *Advanced Quantum Technologies* **4** (2021).
- [16] R. Martínez-Peña, G. L. Giorgi, J. Nokkala, M. C. Soriano, and R. Zambrini, *Dynamical phase transitions in quantum reservoir computing*, *Phys. Rev. Lett.* **127** (2021).
- [17] K. Kobayashi and Y. Motome, *Quantum reservoir probing of quantum phase transitions*, arXiv:2402.07097 (2024).
- [18] A. Sannia, R. Martínez-Peña, M. C. Soriano, G. L. Giorgi, and R. Zambrini, *Dissipation as a resource for quantum reservoir computing*, *Quantum* **8**, 1291 (2024).
- [19] N. Götting, S. Wilksen, A. Steinhoff, F. Lohof, and C. Gies, *Connection between memory performance and optical absorption in quantum reservoir computing*, arXiv:2501.15580 (2025).
- [20] K. Cheamsawat and T. Chotibut, *Dissipation alters modes of information encoding in small quantum reservoirs near criticality*, *Entropy* **27**, 88 (2025).
- [21] G. Llodrà, P. Mujal, R. Zambrini, and G. L. Giorgi, *Quantum reservoir computing in atomic lattices*, *Chaos, Solitons & Fractals* **195**, 116289 (2025).
- [22] J. García-Beni, G. Luca Giorgi, M. C. Soriano, and R. Zambrini, *Squeezing as a resource for time series processing in quantum reservoir computing*, *Optics Express* **32**, 6733 (2024).
- [23] A. Sannia, G. L. Giorgi, S. Longhi, and R. Zambrini, *Liouillian skin effect in quantum neural networks*, *Optica Quantum* **3**, 189 (2025).
- [24] N. Götting, F. Lohof, and C. Gies, *Exploring quantumness in quantum reservoir computing*, *Physical Review A* **108** (2023).
- [25] P. Mujal, R. Martínez-Peña, G. L. Giorgi, M. C. Soriano, and R. Zambrini, *Time-series quantum reservoir computing with weak and projective measurements*, *npj Quantum Information* **9** (2023).
- [26] G. Franceschetto, M. Płodzień, M. Lewenstein, A. Acín, and P. Mujal, *Harnessing quantum back-action for time-series processing*, arXiv:2411.03979 (2024).
- [27] A. Palacios, R. Martínez-Peña, M. C. Soriano, G. L. Giorgi, and R. Zambrini, *Role of coherence in many-body quantum reservoir computing*, *Communications Physics* **7** (2024).
- [28] F. Hu, S. A. Khan, N. T. Bronn, G. Angelatos, G. E. Rowlands, G. J. Ribeill, and H. E. Türeci, *Overcoming the coherence time barrier in quantum machine learning on temporal data*, *Nature Communications* **15** (2024).
- [29] H.-P. Breuer, E.-M. Laine, J. Piilo, and B. Vacchini, *Colloquium: Non-Markovian dynamics in open quantum systems*, *Reviews of Modern Physics* **88** (2016).
- [30] A. Rivas and S. F. Huelga, *Open quantum systems*, Vol. 10 (Springer, 2012).
- [31] I. De Vega and D. Alonso, *Dynamics of non-Markovian open quantum systems*, *Reviews of Modern Physics* **89**, 015001 (2017).
- [32] D. Chruściński, *Dynamical maps beyond Markovian regime*, *Physics Reports* **992**, 1 (2022).
- [33] B.-H. Liu, L. Li, Y.-F. Huang, C.-F. Li, G.-C. Guo, E.-M. Laine, H.-P. Breuer, and J. Piilo, *Experimental control of the transition from Markovian to non-Markovian dynamics of open quantum systems*, *Nature Physics* **7**, 931–934 (2011).
- [34] H.-P. Breuer, E.-M. Laine, and J. Piilo, *Measure for the degree of non-Markovian behavior of quantum processes in open systems*, *Phys. Rev. Lett.* **103**, 210401 (2009).
- [35] J.-S. Xu, C.-F. Li, M. Gong, X.-B. Zou, C.-H. Shi, G. Chen, and G.-C. Guo, *Experimental demonstration of photonic entanglement collapse and revival*, *Phys. Rev. Lett.* **104**, 100502 (2010).
- [36] Y. Wang, Z.-Y. Hao, J.-K. Li, Z.-H. Liu, K. Sun, J.-S. Xu, C.-F. Li, and G.-C. Guo, *Observation of non-Markovian evolution of Einstein-Podolsky-Rosen steering*, *Phys. Rev. Lett.* **130**, 200202 (2023).
- [37] F. Buscemi, R. Gangwar, K. Goswami, H. Badhani, T. Pandit, B. Mohan, S. Das, and M. N. Bera, *Causal and noncausal revivals of information: A new regime of non-Markovianity in quantum stochastic processes*, *PRX Quantum* **6**, 020316 (2025).
- [38] A. W. Chin, S. F. Huelga, and M. B. Plenio, *Quantum metrology in non-Markovian environments*, *Phys. Rev. Lett.* **109**, 233601 (2012).
- [39] D. M. Reich, N. Katz, and C. P. Koch, *Exploiting non-Markovianity for quantum control*, *Scientific Reports* **5** (2015).
- [40] E.-M. Laine, H.-P. Breuer, and J. Piilo, *Nonlocal memory effects allow perfect teleportation with mixed states*, *Scientific Reports* **4** (2014).
- [41] B. Bylicka, D. Chruściński, and S. Maniscalco, *Non-Markovianity and reservoir memory of quantum channels: a quantum information theory perspective*, *Scientific Reports* **4** (2014).
- [42] Y. Dong, Y. Zheng, S. Li, C.-C. Li, X.-D. Chen, G.-C. Guo, and F.-W. Sun, *Non-Markovianity-assisted high-fidelity Deutsch-Jozsa algorithm in diamond*, *npj Quantum Information* **4** (2018).
- [43] M. Thorwart, J. Eckel, J. Reina, P. Nalbach, and S. Weiss, *Enhanced quantum entanglement in the non-Markovian dynamics of biomolecular excitons*, *Chemical Physics Letters* **478**, 234–237 (2009).
- [44] G. Karpat, I. Yalçinkaya, B. Çakmak, G. L. Giorgi, and R. Zambrini, *Synchronization and non-Markovianity in open quantum systems*, *Physical Review A* **103** (2021).

- [45] M. A. C. Rossi, M. Cattaneo, M. G. A. Paris, and S. Maniscalco, *Non-Markovianity is not a resource for quantum spatial search on a star graph subject to generalized percolation*, Quantum Measurements and Quantum Metrology **5**, 40–49 (2018).
- [46] V. Gorini, A. Kossakowski, and E. C. G. Sudarshan, *Completely positive dynamical semigroups of n -level systems*, Journal of Mathematical Physics **17**, 821 (1976).
- [47] G. Lindblad, *On the generators of quantum dynamical semigroups*, Communications in Mathematical Physics **48**, 119 (1976).
- [48] See supplemental material for the proofs of the analytical results presented and for further details on the numerical methods and on the embedded non-Markovian model.
- [49] I. B. Yildiz, H. Jaeger, and S. J. Kiebel, *Re-visiting the echo state property*, Neural Networks **35**, 1–9 (2012).
- [50] S. Boyd and L. Chua, *Fading memory and the problem of approximating nonlinear operators with Volterra series*, IEEE Transactions on Circuits and Systems **32**, 1150–1161 (1985).
- [51] J. Dambre, D. Verstraeten, B. Schrauwen, and S. Massar, *Information processing capacity of dynamical systems*, Scientific Reports **2** (2012).
- [52] A. Ceni and C. Gallicchio, *Residual echo state networks: Residual recurrent neural networks with stable dynamics and fast learning*, Neurocomputing **597**, 127966 (2024).
- [53] S. Chang, Y. Zhang, W. Han, M. Yu, X. Guo, W. Tan, X. Cui, M. Witbrock, M. Hasegawa-Johnson, and T. S. Huang, *Dilated recurrent neural networks*, arXiv:1710.02224 (2017).
- [54] G. Fette and J. Eggert, *Short term memory and pattern matching with simple echo state networks*, in *Artificial Neural Networks: Biological Inspirations – ICANN 2005* (Springer Berlin Heidelberg, 2005) p. 13–18.
- [55] S. Bay, P. Lambropoulos, and K. Mølmer, *Atom-atom interaction in strongly modified reservoirs*, Physical Review A **55**, 1485–1496 (1997).
- [56] A. Imamoglu, *Stochastic wave-function approach to non-Markovian systems*, Physical Review A **50**, 3650–3653 (1994).
- [57] B. M. Garraway, *Nonperturbative decay of an atomic system in a cavity*, Physical Review A **55**, 2290–2303 (1997).
- [58] B. M. Garraway and P. L. Knight, *Cavity modified quantum beats*, Physical Review A **54**, 3592–3602 (1996).
- [59] H.-P. Breuer, *Genuine quantum trajectories for non-Markovian processes*, Physical Review A **70** (2004).
- [60] E. Arrigoni, M. Knap, and W. von der Linden, *Nonequilibrium dynamical mean-field theory: An auxiliary quantum master equation approach*, Phys. Rev. Lett. **110** (2013).
- [61] A. Dorda, M. Nuss, W. von der Linden, and E. Arrigoni, *Auxiliary master equation approach to nonequilibrium correlated impurities*, Physical Review B **89** (2014).
- [62] S. Rijavec and G. Di Pietra, *Tunable non-Markovian dynamics in a collision model: an application to coherent transport*, New Journal of Physics **27**, 043003 (2025).
- [63] M. C. Mackey and L. Glass, *Oscillation and chaos in physiological control systems*, Science **197**, 287–289 (1977).
- [64] J. D. Farmer and J. J. Sidorowich, *Predicting chaotic time series*, Phys. Rev. Lett. **59**, 845 (1987).
- [65] H. Jaeger and H. Haas, *Harnessing nonlinearity: Predicting chaotic systems and saving energy in wireless communication*, Science **304**, 78 (2004).
- [66] S. Ortín, M. C. Soriano, L. Pesquera, D. Brunner, D. San-Martín, I. Fischer, C. R. Mirasso, and J. M. Gutiérrez, *A unified framework for reservoir computing and extreme learning machines based on a single time-delayed neuron*, Scientific Reports **5** (2015).
- [67] A. Weigend and N. Gershenfeld, in *IEEE International Conference on Neural Networks* (1993) pp. 1786–1793 vol.3.
- [68] A. Senanian, S. Prabhu, V. Kremenetski, S. Roy, Y. Cao, J. Kline, T. Onodera, L. G. Wright, X. Wu, V. Fatemi, and P. L. McMahon, *Microwave signal processing using an analog quantum reservoir computer*, Nature Communications **15** (2024).
- [69] J. Chen, H. I. Nurdin, and N. Yamamoto, *Temporal information processing on noisy quantum computers*, Physical Review Applied **14** (2020).
- [70] F. Verstraete, M. M. Wolf, and J. Ignacio Cirac, *Quantum computation and quantum-state engineering driven by dissipation*, Nature Physics **5**, 633–636 (2009).
- [71] L. Buitinck, G. Louppe, M. Blondel, F. Pedregosa, A. Mueller, O. Grisel, V. Niculae, P. Prettenhofer, A. Gramfort, J. Grobler, R. Layton, J. Vanderplas, A. Joly, B. Holt, and G. Varoquaux, *API design for machine learning software: experiences from the scikit-learn project*, arXiv:1309.0238 (2013).

SUPPLEMENTAL MATERIAL FOR “NON-MARKOVIANITY AND MEMORY ENHANCEMENT IN QUANTUM RESERVOIR COMPUTING”

I. VOLTERRA SERIES SCALING FOR A MARKOVIAN QUANTUM RESERVOIR

Following the main text, we study a quantum reservoir model that evolves according to the equation

$$\rho_{k+1} = e^{\mathcal{L}(\vec{s}_{k+1})\Delta t} \rho_k.$$

Considering now the Liouvillian notation where any linear operator is vectorized $\rho \rightarrow |\rho\rangle\rangle$, we can expand $e^{\mathcal{L}(\vec{s}_k)\Delta t}$ in the basis of the $\mathcal{L}(\vec{s}_k)$ eigenvectors:

$$e^{\mathcal{L}(\vec{s}_k)\Delta t} = \frac{|\rho_{ss}(\vec{s}_k)\rangle\rangle\langle\langle\mathbb{I}|}{\langle\langle\mathbb{I}|\rho_{ss}(\vec{s}_k)\rangle\rangle} + \sum_{i=1}^{4^N-1} e^{\lambda_i\Delta t} \frac{|r_i\rangle\rangle\langle\langle l_i|}{\langle\langle l_i|r_i\rangle\rangle} \quad (\text{S1})$$

where the underlying dot product is the Hilbert-Schmidt one: $\langle\langle\tau|\rho\rangle\rangle = \text{Tr}\{\tau^\dagger\rho\}$, \mathbb{I} is the identity operator, $\rho_{ss}(\vec{s}_k)$ is the unique Liouvillian stationary state, $\{\lambda_i\}$ are the non zero Liouvillian eigenvalues, and $\{|r_i\rangle\rangle\}$ and $\{|l_i\rangle\rangle\}$ are corresponding right and left eigenvectors.

All the terms in Eq. (S1) are, in general, input-dependent and all the expansion can be thought of as the sum of two superoperators:

$$e^{\mathcal{L}(\vec{s}_k)\Delta t} = \mathcal{S}(\vec{s}_k) + \mathcal{T}(\vec{s}_k) \quad (\text{S2})$$

where $\mathcal{S}(\vec{s}_k) = \frac{|\rho_{ss}(\vec{s}_k)\rangle\rangle\langle\langle\mathbb{I}|}{\langle\langle\mathbb{I}|\rho_{ss}(\vec{s}_k)\rangle\rangle}$ and $\mathcal{T}(\vec{s}_k)$ is equal to the sum of all the remaining terms.

It is worth noting that for any pair of inputs, \vec{s} and \vec{w} , the following properties hold:

1. $\mathcal{S}(\vec{s})\mathcal{S}(\vec{w}) = \mathcal{S}(\vec{s})$
2. $\mathcal{S}(\vec{s})\mathcal{T}(\vec{w}) = 0$

where the first identity immediately follows from the definition of \mathcal{S} while the second is a consequence of the fact that the right eigenvectors of \mathcal{L} are always traceless.

Given an initial state ρ_{in} and a length L input series $\{\vec{s}_k\}_{k=1}^L$, we can now write the corresponding final state ρ_f :

$$\begin{aligned} \rho_f &= \prod_k e^{\mathcal{L}(\vec{s}_k)\Delta t} \rho_{in} = \prod_k \left(\mathcal{S}(\vec{s}_k) + \mathcal{T}(\vec{s}_k) \right) \rho_{in} \\ &= \prod_{k=1}^L \mathcal{T}(\vec{s}_k) \rho_{in} + \sum_{k'=1}^L \prod_{k>k'} \mathcal{T}(\vec{s}_k) \mathcal{S}(\vec{s}_{k'}) \rho_{in}. \end{aligned} \quad (\text{S3})$$

Given a generic operator norm $\|\cdot\|$, the validity of the echo state property for a Markovian map corresponds to the condition $\|\mathcal{T}(\vec{s})\| < 1$ for any \vec{s} (see Appendix C of [18]) and, as we will now show, it dictates a restriction on the Volterra series of reservoir outputs.

For any output observable $\hat{\mathcal{O}}_i$, a direct application of Eq. (S3) allows finding a useful expression for the $\hat{\mathcal{O}}_i$ expectation value after the application of an infinite inputs sequence:

$$\begin{aligned} \text{Tr}\{\hat{\mathcal{O}}_i \rho_k\} &= \text{Tr}\{\hat{\mathcal{O}}_i (\mathcal{S}(\vec{s}_k) + \mathcal{T}(\vec{s}_k) \mathcal{S}(\vec{s}_{k-1}) + \dots) \rho_{in}\} \\ &= \text{Tr}\{\hat{\mathcal{O}}_i (\mathcal{S}(\vec{s}_k) + \sum_{i=1}^{\infty} \prod_{j=0}^{i-1} \mathcal{T}(\vec{s}_{k-j}) \mathcal{S}(\vec{s}_{k-i})) \rho_{in}\}. \end{aligned}$$

We now notice that a generic functional $f_n(\vec{s}_{k-\tau_1}, \dots, \vec{s}_{k-\tau_n})$, as defined in Eq. (3) of the main text, is the linear combination, for all the output observables $\hat{\mathcal{O}}_i$, of the terms

$$\text{Tr}\{\hat{\mathcal{O}}_i \left(\sum_{i=\tau_n}^{\infty} \prod_{j=0}^{i-1} \mathcal{T}(\vec{s}_{k-j}) \mathcal{S}(\vec{s}_{\tau_n-i}) \right) \rho_{in}\},$$

whose absolute value, as a consequence of Cauchy-Schwarz inequality, is $\mathcal{O}(e^{-a\tau_n})$ with $e^{-a} = \max_{\vec{s}} \|\mathcal{T}(\vec{s})\|$. We can now directly conclude that

$$|f_n(\vec{s}_{k-\tau_1}, \dots, \vec{s}_{k-\tau_n})| = \mathcal{O}(e^{-a\tau_n}),$$

as claimed in the main text.

II. NUMERICAL METHODS

In the following, we give the details about the numerical results presented in the main text. In all the tasks considered, and for each reservoir model studied, we computed the performance values across 100 multiple realizations to obtain results that are not affected by statistical variability. In particular, we evaluated the performance average varying the initial conditions of the reservoir state and Hamiltonian samples. Moreover, in the case of random inputs, this statistical average also took into account the input sequence randomness. Before measuring performance, we let the reservoir evolve for 1000 time steps under the given input sequence to eliminate the dependence on initial conditions (washout phase), ensuring the validity of the echo state property [15]. Following this, 1000 data points were used to train the output layer's free parameters (training phase) [12].

Numerically, we utilized the *scikit-learn* library [71] to determine the optimal weights $\{w_i\}_i$, as defined in the main text. In particular, these weights were obtained by minimizing the following least squares error during the training phase:

$$\sum_k (y_k - \hat{y}_k)^2,$$

where k indexes the training steps, and y_k and \hat{y}_k represent the reservoir output series and the target series value, respectively, following the notation introduced in the main text.

Moreover, once the training was completed, we evaluated the performance in a subsequent test phase on the 1000 following points of the reservoir dynamics. In the tasks evaluated with the capacity, we computed its value by adapting Eq. (5) of the main text to the case of mono-dimensional reservoir outputs [51]:

$$C = \frac{\text{cov}^2(y, \hat{y})}{\sigma(y)^2 \sigma(\hat{y})^2}$$

where y and \hat{y} respectively refer to series of reservoir outputs and target values; cov indicates the covariance; and σ is the standard deviation.

III. DETAILS ON THE EMBEDDED NON-MARKOVIAN MODEL

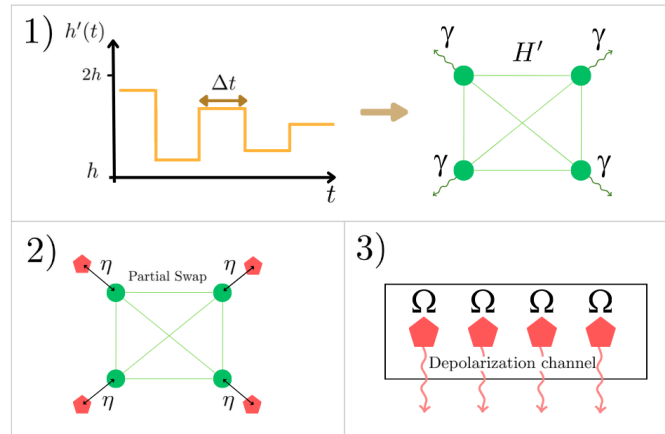


FIG. S1. Schematic representation of the main steps in the evolution rule of the embedded non-Markovian model presented in the main text: (1) Input is injected through Hamiltonian driving in the Lindbladian; (2) interaction with auxiliary qubits occurs via partial swaps; (3) depolarizing channels act on the auxiliary qubits to tune the degree of non-Markovianity.

We now proceed to provide some details on the embedded non-Markovian model introduced in the main text (See Fig. S1 for a schematic summary of the model). In particular, we will numerically quantify its non-Markovianity level, varying Ω and fixing the same hyperparameter used in the main text. Moreover, we will study its past inputs memory evaluating the short-term memory task, defined in the main text.

A. Characterization of non-Markovianity

To quantify the amount of non-Markovianity, as the reservoir dynamics are described by a map that consists of discrete steps, we follow the discrete measure introduced in [34]:

$$\mathcal{N} = \max_{\{\rho_{0,1}, \rho_{0,2}\}} \sum_{k \in \Sigma_+} (D(\rho_{k,1}, \rho_{k,2}) - D(\rho_{k-1,1}, \rho_{k-1,2})), \quad (\text{S4})$$

where $\rho_{k,1}$ and $\rho_{k,2}$ denote the k -th reservoir states corresponding to two different initial conditions, respectively $\rho_{0,1}$ and $\rho_{0,2}$. Moreover, the summation is only taken for the values of k that fulfill the condition

$$D(\rho_{k,1}, \rho_{k,2}) - D(\rho_{k-1,1}, \rho_{k-1,2}) > 0,$$

with

$$D(\rho_1(t), \rho_2(t)) = \frac{1}{2} \|\rho_1(t) - \rho_2(t)\|_1,$$

where $\|\cdot\|_1$ is the trace distance.

We numerically estimate the maximum of the summations of Eq. (S4) by computing 100 sums, randomly varying the reservoir Hamiltonian, the initial reservoir states, and the input series. Moreover, the number of time steps used in the computation has been considered to be 1000, corresponding to the number of points in the washout phase. In fact, after the washout phase, it has been numerically found that the reservoir states are practically initial-state independent, giving negligible contributions to Eq. (S4).

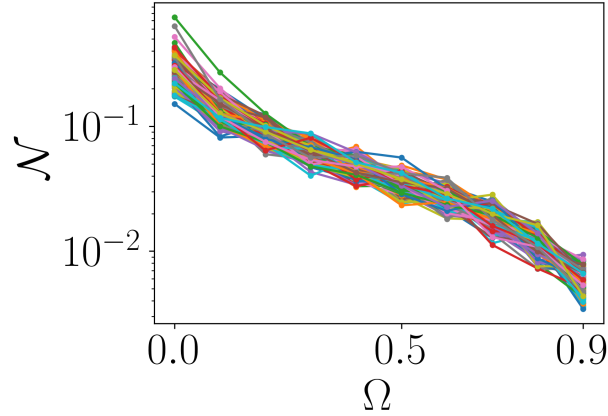


FIG. S2. Non-Markovianity measure as a function of Ω in logarithmic scale. 100 random realizations of the sum in Eq. (S4) have been depicted, varying reservoir Hamiltonian, initial states, and the input series. The case of $\Omega = 1$ has not been represented because the corresponding values are equal to zero up to numerical round-off errors. As in the main text, the remaining hyperparameters are: $h = 1$, $dt = 0.5$, $\gamma = 0.1$, $\eta = \pi/4$ and $2N = 8$.

In Fig. S2, we show the computed sums as a function of Ω . As we can see, they tend to monotonic decrease w.r.t. Ω , suggesting that Ω is a good variable to tell the non-Markovianity amount.

B. Short-term memory task

Following the main text, we now evaluate the performance of the short-term memory task for the embedded non-Markovian reservoir, using the criteria explained in the numerical methods section, to study the reservoir memory behaviour.

From Fig. S3, we conclude that the Markovian case ($\Omega = 1$) leads to capacity decay, as predicted by our theoretical results. In contrast, the non-Markovian regime ($\Omega = 0$, $\Omega = 0.5$) exhibits memory revivals. Notably, when $\Omega = 0$, despite the presence of these revivals, the reservoir maintains weak correlations with past inputs. This behavior helps explain the performance of Mackey-Glass series predictions, as discussed in the main text. Specifically, only when $\Omega = 0.5$, the non-Markovian dynamics enhance the reservoir's correlation with past inputs.

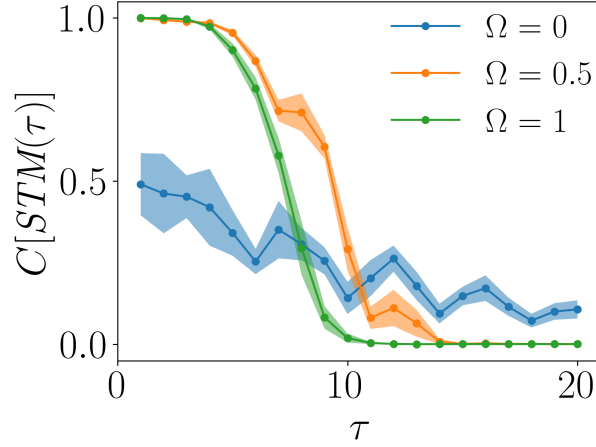


FIG. S3. Capacity of the short-term memory task as a function of the delay τ , considering different Ω values. The shadow regions cover one standard deviation calculated randomly varying the Hamiltonian, the initial reservoir state, and the injected sequence. According to the main text, the other hyperparameters have been fixed to: $h = 1$, $dt = 0.5$, $\gamma = 0.1$, $\eta = \pi/4$ and $2N = 8$.

C. Sante Fe series task

The Santa Fe series prediction task is a well-established benchmark for evaluating the performance of nonlinear time series forecasting models. It was introduced at a time series competition, organized by the Santa Fe Institute in the early 1990s [67]. The dataset consists of intensity measurements from a laser system operating in a chaotic regime. Driving the reservoir with these values, rescaled in range $[0, 1]$ and indicated with $\{s_k\}_k$, the studied task formally consists of reproducing the target series

$$\hat{y}_k(\eta) = s_{k+\eta},$$

where η is the number of steps forward in the prediction.

The reservoir was trained and its performance evaluated as outlined in the previous section. The results of the Santa Fe prediction task are presented in Fig. S4. Different from the Mackey-Glass forecasting task studied in the main text, we notice that, in this case, no significant improvement was found in working in a non-Markovian regime ($\Omega \neq 1$). We can justify this by noting that in the Santa Fe task, the inputs into the reservoir are always the true values from the intensity measurements dataset. In contrast, in the Mackey-Glass case, the system, in the testing phase, is left to evolve autonomously, making the task more demanding.

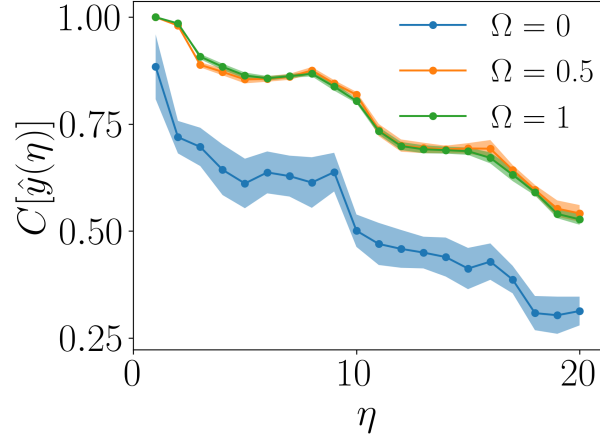


FIG. S4. Capacity of the Santa Fe task as a function of η , varying the value of Ω . The shadow regions cover one standard deviation calculated with respect to the Hamiltonian realizations and the initial reservoir states. As the reservoir model studied in the main text, the hyperparameters have been fixed to: $h = 1$, $dt = 0.5$, $\gamma = 0.1$, $\eta = \pi/4$ and $2N = 8$.